Draft: *ChemSelect*, 2021, *6(12)*, 2975-2979.

Quantitative PCR of Small Nucleic Acids: Size Matters

Jay Min Lim,[a] Rahul Tevatia,*[a] and Ravi F. Saraf*[b]

[a] J. M. Lim, Dr. R. Tevatia,
Vajra Instruments Inc.,
8300 Cody Drive, Ste C,
Lincoln, NE 68512 (USA)
E-mail: rahul.tevatia@vajrainstruments.com

[b] Prof. Dr. R. F. Saraf
Department of Chemical and Biomolecular Engineering,
University of Nebraska-Lincoln,
Lincoln NE 68588 (USA)
E-mail: rsaraf2@unl.edu

Table of Content

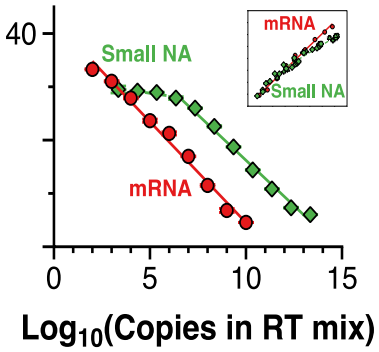

Amplicon length limits the qPCR quantification of small nucleic acids (NA). The limitation of current quantitative PCR methodologies for small nucleic acids quantification is studied using commercial kits. Using pristine molecules, the limit of quantification of small NA is in picomolars which is over three orders of magnitude lower than long mRNA in femtomolars, as expected. The difference is attributed primarily to the size of the amplicon during quantitative PCR reaction.

Quantitative PCR of Small Nucleic Acids: Size Matters

Jay Min Lim,[a] Rahul Tevatia,*[a] and Ravi F. Saraf*[b]

[a] J. M. Lim, Dr. R. Tevatia,
Vajra Instruments Inc.,
8300 Cody Drive, Ste C,
Lincoln, NE 68512 (USA)
E-mail: rahul.tevatia@vajrainstruments.com

[b] Prof. Dr. R. F. Saraf
Department of Chemical and Biomolecular Engineering,
University of Nebraska-Lincoln,
Lincoln NE 68588 (USA)
E-mail: rsaraf2@unl.edu

ABSTRACT

Quantitative dysregulation in small nucleic acids (NA), such as microRNA (miRNA), extracted from minimally invasive biopsies, such as, blood, stool, urine, nose, throat, are promising biomarker for diseases diagnosis and management. We quantify the effect of the extra step of poly(A) ligation for cDNA synthesis and small size of the NA on the limit of quantification (LOQ) of quantitative PCR (qPCR), the gold standard to measure copy number. It was discovered that for small NA, the cycle threshold, Ct that is proportional to -log[c], where [c] is the concentration of the target NA exhibits a sharp transition. The results indicate that although the limit of detection (LOD) of qPCR can be in femtomolar range, the LOQ is significantly reduced by well over three orders of magnitude, in picomolar range. Specifically, the study reveals that the PCR product length is the primary reason the limitation on LOQ and is explicitly shown to be an important consideration for primer design for qPCR in general.

Introduction

Quantitative genomics to measure copy number of specific nucleic acid (NA) sequences in non-invasively obtained biospecimens, i.e., liquid biopsy,[1] is rapidly coming to center stage[2] as a diagnostic and prognostic tool for cancer,[3] heart,[4] psychiatric,[5] and infectious[6] diseases, among others. The viral load of SARS-CoV2 in nasal swab samples by measuring copy number of viral RNA is central to discerning contagiousness and contact tracing.[7] Dysregulation in copy number of circulating noncoding RNA (ncRNA),[8] particularly, microRNA (miRNA), are shown to be effective biomarkers for cancer for early stage detection and disease management.[9] An important need emerging is quantification of small, less than ~50 nucleotide (nt) long NA's which does not have a poly(A)-tail present at the 3'-end for mRNA.

Quantitative Polymerase Chain Reaction (qPCR) is considered the gold standard for relative or absolute measurement of copy number of specific sequence in a

biospecimen.[10] Complimentary DNA (cDNA) are synthesized for each NA molecule using a reverse transcriptase (RT) enzyme in a thermal cycler; followed by qPCR where the cDNA is replicated in a cyclic process.[11] The number of copies nominally double during each cycle controlled by periodic temperature excursion leading to amplification curves that are measured by fluorescence that is exclusively caused by a dye that intercalates in the PCR product.[11] In qPCR, the copy number of the original NA molecules is calculated from the number of cycles needed in the qPCR to obtain a threshold number of copies, cycle threshold Ct.[11] The Ct is proportional to -klog[N], where N are the number of target (cDNA) molecules in qPCR reaction mixture and k is the slope of the so called qPCR standard curve. From simple geometric growth at efficiency, E for each amplification cycle, $E = 10^{(-1/k)} - 1$, thus for E =1, k ~ -3.32.[12] The quantitative range of qPCR is defined as the range where the exponential relationship holds, i.e., k is constant. Furthermore, to obtain quantification of the copies in the original sample, i.e., number of copies in the RT mix to form cDNA, it is generally assumed that the efficiency of cDNA synthesis is close to 100%, i.e., for each copy of target NA one copy of cDNA is synthesized. An aspect of the study reported is quantitatively access the efficiency of NA to cDNA conversion.

Since the discovery of qPCR over 25 years ago,[13] continual effort on developing better algorithms to analyze the measured Ct to accurately and reliably quantify the copy number of NA is a testimony to the complexity and challenges.[14] For example, “kit-dependent” conditions lead to high variability and data bias making intra- and inter-lab results irreproducible causing great debate and frustration.[15] Thus, the need for standardization of PCR assay is well recognized.[16] There is ample evidence that the choice of primer is crucial in designing proper quantitative analysis by qPCR.[12] Here we focus on two additional consideration for qPCR analysis to quantify copy number particularly of small NA. The premise of the study is our central observation that the limit of quantification (LOQ) of small NA compared to (long) standard mRNA as a control, is orders of magnitude lower (discussed in Fig. 2). To explain this drastic reduction in LOQ we identify A-tail ligation and qPCR amplicon length as two primary factors, where the second one is more significant and has not been explicitly realized. First, the ligation of poly(A)-tail that is essential for cDNA synthesis that is missing in small ncRNA, including a range of long noncoding RNA (lncRNA).[17] Second, the small size of the NA will limit the binding site of the primer molecules for amplification is roughly (only) 6-8 nt.[18] The length of the binding site may limit the specificity to differentiate miRNA families with only a few changes in bases,[19] that may not be in the primer binding site. The key finding is that the small product size during the qPCR amplification also called the amplicon, rather than the ligation step for cDNA synthesis, is the primary reason to significantly decrease the LOQ of qPCR by over three orders of magnitude. Although, our analysis is focused on SYBR Green based method that are significantly more inexpensive and pervasive than the TaqMan method,[20] the key observation on the limitations and recommendations are similar.

Results and Discussion

The result for the first consideration, effect of cDNA synthesis which includes A-tail ligation, is discussed. To quantify the effect of poly(A)-tail ligation on small NA, two approaches were adopted to relate the Ct value to the copy number (N) of starting ssDNA or RNA (Fig. 1): Method ① (Target Dilution): The original stock, $N_1 = 10^{13}$ copies is diluted to different amounts, d_1N_1, where d_1 is dilution amount followed by cDNA synthesis (which includes poly(A)-tail ligation) at efficiency, η_1. The qPCR is performed on $(N_1d_1)\eta_1$. Method ② (cDNA Dilution): The cDNA is synthesized from $N_2 = 10^{13}$ copies in RT mix at efficiency, η_2, and then diluted by d_2. The qPCR is performed on $(N_2\eta_2)d_2$. (To note is that, for clarity, the order of the variables is to reflect the sequence of process steps). To quantitatively examine if the overall efficiency of poly(A)-tail ligation and cDNA synthesis changes at lower number of molecules in RT mix, η_1 and η_2 are compared by setting $N_1d_1 = N_2d_2$. If the efficiency of A-tail ligation and cDNA synthesis is larger in cDNA dilution approach, i.e., $\eta_2 > \eta_1$, then Ct_1 will be larger than Ct_2, and vice versa. In case the cDNA conversion efficiency is unchanged for all number of molecules in RT mix, i.e., both methods have same efficiency ($\eta_1 = \eta_2$), then, $Ct_1 = Ct_2$.

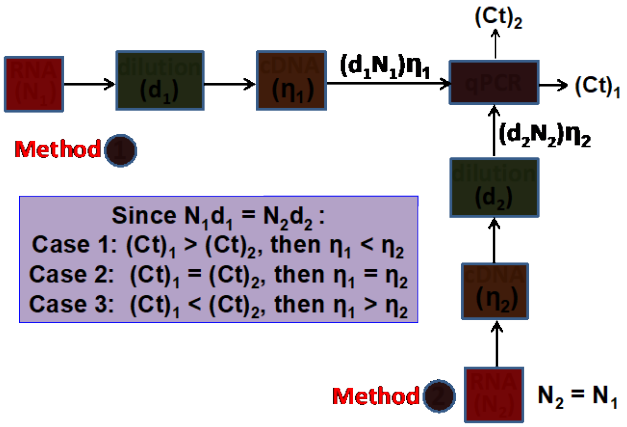

Figure 1. *Flow chart for cDNA synthesis and qPCR analysis*. The copy numbers are measured by two methods: (a) Nucleic acid dilution (Method ①); and cDNA dilution (Method ②).

The standard curves for miR-34a and miR-155, detailed in SI, Table S1, were measured by both the dilution methods (Fig. 2). The standard curves for miR-34a and miR-155 in both RNA and DNA form are significantly different from Luciferase Control mRNA (as this is the only mRNA in our study, from now on, we will refer it as just 'mRNA') (Fig. 2). The sequences of the primer pair targeting mRNA (Primer Set 4) is in SI, Table S2. The mRNA shows an expected standard curve with slope, k = -3.76 which is slightly lower than the expected range,[12] corresponding to E ~ 85%. The LOQ for mRNA defined as the lowest measurable copies in the exponential region was Ct ~ 35 corresponds to N ~

10^2 copies in the RT mix which is consistent with the "best practice" methods.[21] In terms of concentration, the LOQ corresponded to [c] ~16.7 fM in the (starting) sample. Furthermore, as expected, the results are virtually identical for the two dilution approaches. The high coincidence for the two dilution approaches over eight orders of magnitude clearly indicates that for mRNA, $\eta_2 = \eta_1 = 1$, i.e., the efficiency of cDNA synthesis is 100%. The corresponding melt curves for the qPCR shows the required single peak of the product at Tm ~ 84.8°C (SI Fig. S1). Thus, the behavior for mRNA serves as a control indicating that the two dilution methods are equivalent and there are no spurious errors in sample handling and processing, such as, pipetting, NA storage, buffer exchanges between various processes.

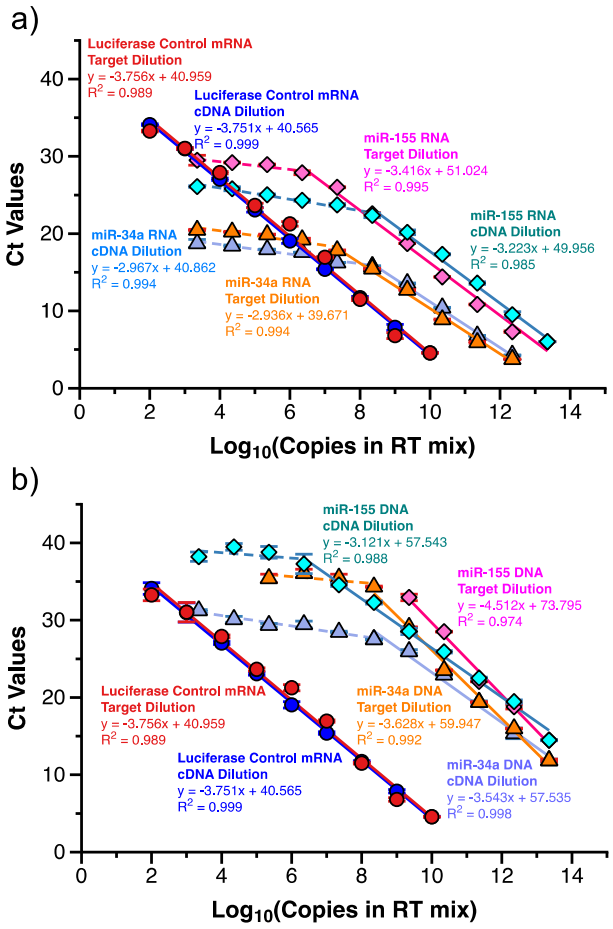

Figure 2. *Comparison of standard curves for NA studied*. Standard curves based on a) RNA form, and b) DNA form of respective miRNA. Control is standard curve of Luciferase mRNA. Based on Fig. 1, the number of copies in RT mix for Method ① and Method ② were N_1d_1 and N_2 for the two methods. Thus, to normalize for dilution effect in Method ②, the number of equivalent copies in the RT mix are shown, i.e., N_1d_1 and N_2d_2.

For small NA targets, processed in parallel with mRNA on the same well plate, the standard curve is remarkably different from mRNA in two salient aspects (Fig. 2): (i) the LOQ is significantly reduced by well over three to six orders of magnitude as signified by the large shift to the right of the exponential line; and (ii) the Ct value plateaus at lower NA target copies. Although the LOQ is low, the limit of detection (LOD), defined as the highest measurable Ct (SI, Fig. S2) where the melt and amplification curves are (still) reasonable (SI, Fig. S3-S6), was ~10^2 to 10^3 copies that is comparable to LOQ and LOD of mRNA (Fig. 2). Furthermore, the slopes of the standard curves are practical reflecting reasonable amplification efficiencies.[12] Importantly, the significantly lower LOQ due to shift and the plateau-like characteristics at high Ct were also observed for TaqMan method further supporting the two above-mentioned aspects for small NA (Fig. 3). Although the LOQ for TaqMan was two orders of magnitude lower than SYBR Green method, it was still significantly lower than that for mRNA in Fig. 2. The LOD for both the methods was comparable and similar to that for mRNA. Lastly, it should be mentioned that the tight error bars based on running each reaction in triplicate for each condition and one peak in melt curve indicate that artifacts due to processing and chemical contamination and any possibility of primer-dimer formation was unlikely for both mRNA and small NA's (SI, Fig. S3-S6).

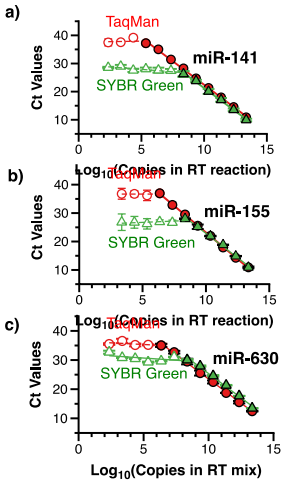

d)

Fit Parameters	TaqMan	SYBR Green
miR-141		
Slope	-3.344	-3.302
Intercept	55.875	54.300
R^2	0.998	0.997
LOQ (Copies in RT mix)	10^5	10^7
LOD (Copies in RT mix)	10^2	10^2
miR-155		
Slope	-3.734	-3.416
Intercept	60.544	57.024
R^2	0.999	0.995
LOQ (Copies in RT mix)	10^6	10^8
LOD (Copies in RT mix)	10^3	10^3
miR-630		
Slope	-3.319	-3.332
Intercept	56.715	58.68
R^2	0.998	0.991
LOQ (Copies in RT mix)	10^6	10^8
LOD (Copies in RT mix)	10^2	10^2

Figure 3. *Standard curves for miRNA using TaqMan method*. (a) to (c) The standard curve for the microRNA for TaqMan and SYBR Green method are compared. (d) Table showing the parameters from the exponential fit and the LOD.

The cDNA synthesis has been recognized as a major source of error depending on the RNA quality[22] and kit utilized for the RT reaction.[23] However, for the pristine mRNA studied here, the characteristics for the two dilution processes for mRNA was virtually identical for over eight orders of magnitude, up to LOQ of N ~10^2 molecules indicating that cDNA synthesis was virtually perfect corresponding to same number of target

molecules in the whole (target) concentration range. In contrast to mRNA, the standard curve for the two dilution methods is not coincident for small NA's (Fig. 2). To quantitatively compare the discrepancy, Ct value for the known initial starting copy number (N_1 or N_2) times the respective dilution (d_1 and d_2) are compared, i.e., Ct values for $N_1d_1 = N_2d_2$. If $\eta_1 = \eta_2$ then the number of copies in qPCR mix, $(N_1d_1)\eta_1$ or $(N_2\eta_2)d_2$ will be the same leading to $Ct_1 = Ct_2$. At lower dilution, indeed $\eta_1 = \eta_2$; however, at larger dilution, Ct_1 for $N_1d_1\eta_1$ copies in the qPCR mix is larger than Ct_2 for $N_2d_2\eta_2$ copies implying, $\eta_1 < \eta_2$ (Fig. 4). The discrepancy suggests that when the efficiency for cDNA conversion decreases (from 100%) as the number of copies in the RT mix reduces. At the extreme, for $Ct_1 \sim 35$ the corresponding $Ct_2 \sim 30$ indicating a reduction in copy number of roughly 10-fold in the qPCR mix for the former (as per Fig. 2(b) for miR-155 DNA). Although, the error of 10-fold is significant, it does not account for three to six order of shift in the standard curve compared to mRNA observed in Fig. 2. Nevertheless, it should be noted that the cDNA synthesis efficiency for low copy number of small NA can decrease by 10-fold.

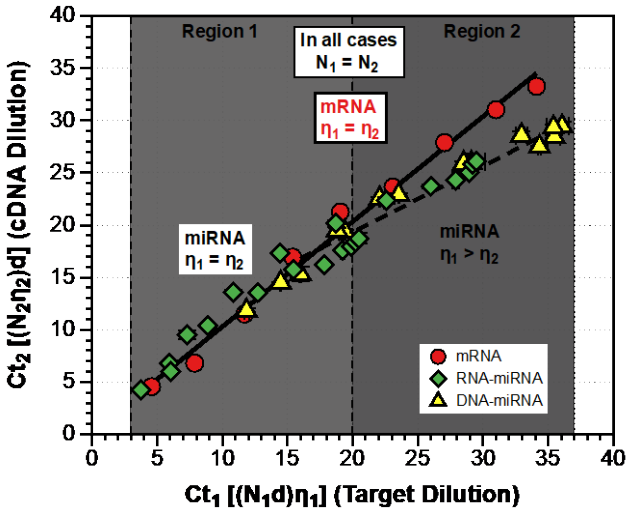

Figure 4. *Effect of dilution on Ct value*. From Fig. 1, the number of copies in qPCR mix to measure Ct value for Method ① and Method ② were, $N_1d_1\eta_1$ and $N_2\eta_2d_2$. Each data point in the plot is for Ct_1 and Ct_2 corresponding N_1d_1 and N_2d_2, respectively. Thus, points for $\eta_1 = \eta_2$ will be on the diagonal.

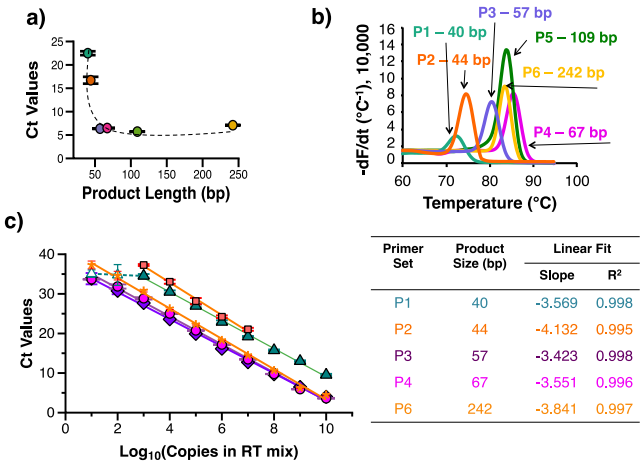

Primer Set	Product Size (bp)	Linear Fit	
		Slope	R^2
P1	40	-3.569	0.998
P2	44	-4.132	0.995
P3	57	-3.423	0.998
P4	67	-3.551	0.996
P6	242	-3.841	0.997

Figure 5. *Effect of qPCR product length on Ct value*. (a) For a fixed amount of Luciferase Control mRNA. (b) The corresponding melt curve of amplified products in (a). P1 and P2 shows Tm ~ 73-75°C, similar to Tm of miRNA amplification (see Fig S3-S6, SI). (c) The corresponding standard curve for primer sets P1 to P5 (see Table S2, SI). (d) The exponential parameters from the standard curves in (c) for each primer set.

To explain the large shift in standard curve and consequently the LOQ for small NA's compared to mRNA, we consider the nature of primers. It is well documented in the literature that selection of the primer is critical in developing an optimum qPCR measurement.[12] However, the effect of primer selection that exclusively affects the length of the amplicon product rather than its location on the mRNA has not been reported. We chose primer set for mRNA to systematically affect the length of the qPCR product length (see SI, Table S2). For fixed number of mRNA copies in RT mix, the resulting Ct value changed significantly (Fig. 5(a)). The number of copies in the RT mix was 10^{10} which was well in the exponential region of the standard curve (Fig. 2). The sudden and remarkable increase in the Ct value for small product length may be explained by considering the fluorescence signal generation in the qPCR to determine the Ct value. SYBR Green measures dsDNA formation (i.e., amplicons) during qPCR reaction due to 10^3-fold enhancement in fluorescence on binding to the duplex.[24] Therefore, the (threshold) fluorescence signal that determines the Ct value will depend on the SYBR Green-dsDNA binding per bp of the amplicon. For higher binding per bp of amplicon, fluorescence threshold will be obtained at low Ct value. The interaction of SYBR Green and dsDNA is by intercalation and minor groove.[25] The electrostatic minor groove binding site occupies about 3-4 bases[25] which may be unaffected by binding per bp of amplicon. However, due to well-known requirement of duplex unwinding to accommodate intercalation in the π-π stacks of bases,[26] the effective inclusion of number of SYBR Green will be limited as the size of the amplicon reduces. The latter is the well-studied neighbor-exclusion principle.[27] As a result, the binding of SYBR Green per dsDNA base-pair, and hence the fluorescence, from small duplex chains will be lower than longer chains. From Fig. 5(a), for product length >50 bp the

intercalation and binding is adequate to efficiently count the number of duplex formations. However, below 50 bp the efficiency starts to rapidly decrease attributed to neighbor-exclusion requiring more number of cycles to make adequate product for substantial increase in fluorescence leading to higher Ct value. The corresponding melt curve indicates single product formation with no side reactions, such as primer-dimer effects (Fig. 5(b). The melt curve for longer products, P3 to P6 for product length >50 bp falls T_m falls within 80–85°C (Fig. 5(b)) that is comparable Luciferase Control mRNA at T_m of ~84.5 ºC (SI, Fig. S1). The no particular trend in T_m as a function of product sizes is attributed to non-systematic differences in GC content and product length. However, the shorter product lengths, have a T_m of 73.2°C (40 bp) and 74.8°C (44 bp) (Fig. 5(b)) which resemble the melt-curves and Tm values of miR-34a (T_m of ~75°C in SI, Figs. S3 and S4) and miR-155 (T_m of ~ 73°C in SI Fig S5 and S6). This indicates that the shorter product length limits the miRNA amplification. Importantly, the higher Ct value for smaller product size leads to significant shift right of the standard curve for larger product size of mRNA. Furthermore, plateau region begins to appear at high Ct value for smaller primer length, P1 primer set (Fig. 5(c)). Thus, we can reasonably attribute the lower LOQ and plateau effect observed in Fig. 2 for small NA to the small qPCR product length. Although not explicitly mentioned in the study, the significant improvement in sensitivity by ligating artificially longer, such as stem-loop chains to miRNA,[18] may be attributed to the chain length effect discovered in this study.

Conclusions

The standard curves of synthetic small NA (~22-25 nt) and reference Luciferase Control mRNA were measured. The standard curves were compared for samples of known dilution of the target NA before cDNA synthesis (i.e., target dilution) to samples where synthesis of cDNA at high concentration was followed by dilution after the RT reaction (cDNA dilution). The standard curve of long mRNA exhibited the expected behavior with LOQ of ~100 copies in the RT mix. The standard curve for target or cDNA dilution was virtually identical over eight orders of magnitude indicating that efficiency of cDNA synthesis from target mRNA was virtually 100%. The qPCR behavior for small NA's was remarkably different. First, the standard curve significantly shifted to the right with respect to mRNA by three to six orders of magnitude leading to well over 10^3-fold higher LOQ than for mRNA. Second the standard curve exhibited a plateau at low concentrations. Third the target and cDNA dilution were different such that at low target concentrations leading to Ct below 20, the efficiency of cDNA synthesis was significantly reduced. The cDNA copies were 10-fold fewer when the Ct for target dilution was about 35. The inferior performance of qPCR on small NA was explained by considering the size of the amplicon in qPCR reaction. In a unique set of experiment, it was observed that if the qPCR product (i.e., amplicon) is below ~50 bp, the LOQ reduces by 10-fold even for mRNA. The effect is attributed to neighbor-exclusion principle. For small qPCR product, a plateau behavior in mRNA similar to small NA is observed. We conclude that while designing the primer sequences, it is important to ensure the length of the qPCR product is above 50 bp. Therefore, for small NA analysis

the cDNA chain length should be long to obtain low LOQ. However, as the ligation chain length increases, the efficiency of cDNA synthesis may decrease.

Supporting Information

Supporting information contains information on miRNA sequences, primers detail, limit of quantification (LOQ) and limit of detection (LOD) of qPCR, amplification and melt curves for Luciferase Control mRNA, miR-34a and miR-155 nucleic acids.

Authors Contribution

R.F.S and R.T. conceived the project and provided guidance on data analysis and interpretation. J.M.L. and R.T. performed experiments, analyzed, and interpreted data. R.F.S., R.T. and J.M.L. wrote the manuscript. R.F.S obtained the financial support for the project.

Acknowledgements

R.F.S. would like to thank NIH/NCI (R44CA199058) and NIH/NHGRI (R43HG010118) for financial support.

Keywords – Intercalations, MicroRNA, Nucleic acids, Polymerase chain reaction, Reverse transcription.

References

[1] a) S. Anfossi, A. Babayan, K. Pantel, G. A. Calin, *Nat. Rev. Clin. Oncol.* **2018**, *15*, 541-563; b) G. Rossi, M. Ignatiadis, *Cancer Res.* **2019**, *79*, 2798.

[2] a) O. Pös, O. Biró, T. Szemes, B. Nagy, *Eur. J. Hum. Genet.* **2018**, *26*, 937-945; b) J. C. M. Wan, C. Massie, J. Garcia-Corbacho, F. Mouliere, J. D. Brenton, C. Caldas, S. Pacey, R. Baird, N. Rosenfeld, *Nat. Rev. Cancer* **2017**, *17*, 223-238.

[3] E. Yong, *Nature* **2014**, *511*, 524-526.

[4] S. H. Kanuri, J. Ipe, K. Kassab, H. Gao, Y. Liu, T. C. Skaar, R. P. Kreutz, *Atherosclerosis* **2018**, *278*, 232-239.

[5] O. Issler, A. Chen, *Nat. Rev. Neurosci.* **2015**, *16*, 201-212.

[6] a) V. M. Corman, O. Landt, M. Kaiser, R. Molenkamp, A. Meijer, D. K. Chu, T. Bleicker, S. Brünink, J. Schneider, M. L. Schmidt, D. G. Mulders, B. L. Haagmans, B. van der Veer, S. van den Brink, L. Wijsman, G. Goderski, J.-L. Romette, J. Ellis, M. Zambon, M. Peiris, H. Goossens, C. Reusken, M. P. Koopmans, C. Drosten, *Euro Surveill.* **2020**, *25*, 2000045; b) E. M. Elnifro, A. M. Ashshi, R. J. Cooper, P. E. Klapper, *Clin. Microbiol. Rev.* **2000**, *13*, 559-570.

[7] X. He, E. H. Y. Lau, P. Wu, X. Deng, J. Wang, X. Hao, Y. C. Lau, J. Y. Wong, Y. Guan, X. Tan, X. Mo, Y. Chen, B. Liao, W. Chen, F. Hu, Q. Zhang, M. Zhong, Y. Wu, L. Zhao, F. Zhang, B. J. Cowling, F. Li, G. M. Leung, *Nat. Med.* **2020**, *26*, 672-675.

[8] A. V. Savelyeva, E. V. Kuligina, D. N. Bariakin, V. V. Kozlov, E. I. Ryabchikova, V. A. Richter, D. V. Semenov, *BioMed Res. Int.* **2017**, *2017*, 7404912.

[9] a) G. De Rubis, S. Rajeev Krishnan, M. Bebawy, *Trends Pharmacol. Sci.* **2019**, *40*, 172-186; b) E. A. Lolomadze, V. V. Kometova, V. V. Rodionov, *Bull. Russ. State Med. Univ.* **2020**, *3*, 5-10.

[10] J. Murphy, S. A. Bustin, *Expert. Rev. Mol. Diagn.* **2009**, *9*, 187-197.

[11] M. Kubista, J. M. Andrade, M. Bengtsson, A. Forootan, J. Jonák, K. Lind, R. Sindelka, R. Sjöback, B. Sjögreen, L. Strömbom, A. Ståhlberg, N. Zoric, *Mol. Aspects Med.* **2006**, *27*, 95-125.

[12] T. Nolan, R. E. Hands, S. A. Bustin, *Nat. Protoc.* **2006**, *1*, 1559-1582.

[13] R. Higuchi, C. Fockler, G. Dollinger, R. Watson, *Nat. Biotechnol.* **1993**, *11*, 1026-1030.

[14] a) A. Forootan, R. Sjöback, J. Björkman, B. Sjögreen, L. Linz, M. Kubista, *Biomol. Detect. Quantif.* **2017**, *12*, 1-6; b) Y. Panina, A. Germond, B. G. David, T. M. Watanabe, *BMC Bioinformatics* **2019**, *20*, 295-295; c) T. D. Schmittgen, K. J. Livak, *Nat. Protoc.* **2008**, *3*, 1101-1108; d) J. Tellinghuisen, A. N. Spiess, *Biomol. Detect. Quantif.* **2019**, *17*, 100084; e) J. S. Yuan, A. Reed, F. Chen, C. N. Stewart, *BMC Bioinformatics* **2006**, *7*, 85.

[15] a) R. T. Hayden, K. M. Hokanson, S. B. Pounds, M. J. Bankowski, S. W. Belzer, J. Carr, D. Diorio, M. S. Forman, Y. Joshi, D. Hillyard, R. L. Hodinka, M. N. Nikiforova, C. A. Romain, J. Stevenson, A. Valsamakis, H. H. Balfour, Jr., U. S. E. W. Group, *J. Clin. Microbiol.* **2008**, *46*, 157-163; b) J. P. Jaworski, A. Pluta, M. Rola-Łuszczak, S. L. McGowan, C. Finnegan, K. Heenemann, H. A. Carignano, I. Alvarez, K. Murakami, L. Willems, T. W. Vahlenkamp, K. G. Trono, B. Choudhury, J. Kuźmak, *J. Clin. Microbiol.* **2018**, *56*, e00304-00318; c) T. Zhang, S. Grenier, B. Nwachukwu, C. Wei, J. H. Lipton, S. Kamel-Reid, S. Association for Molecular Pathology Hematopathology, *J. Mol. Diagn.* **2007**, *9*, 421-430.

[16] a) Stephen A. Bustin, R. Mueller, *Clin. Sci. (Lond.)* **2005**, *109*, 365-379; b) S. A. Bustin, R. Mueller, *Mol. Aspects Med.* **2006**, *27*, 192-223.

[17] Y. Zhang, L. Yang, L. L. Chen, *Int. J. Biochem. Cell Biol.* **2014**, *54*, 338-349.

[18] D. A. Forero, Y. González-Giraldo, L. J. Castro-Vega, G. E. Barreto, *BioTechniques* **2019**, *67*, 192-199.

[19] D. P. Bartel, *Cell* **2009**, *136*, 215-233.
[20] M. Tajadini, M. Panjehpour, S. H. Javanmard, *Adv. Biomed. Res.* **2014**, *3*, 85-85.
[21] S. C. Taylor, K. Nadeau, M. Abbasi, C. Lachance, M. Nguyen, J. Fenrich, *Trends Biotechnol.* **2019**, *37*, 761-774.
[22] S. Bustin, H. S. Dhillon, S. Kirvell, C. Greenwood, M. Parker, G. L. Shipley, T. Nolan, *Clin. Chem.* **2015**, *61*, 202-212.
[23] J.-P. Levesque-Sergerie, M. Duquette, C. Thibault, L. Delbecchi, N. Bissonnette, *BMC Mol. Biol.* **2007**, *8*, 93-93.
[24] H. Zipper, H. Brunner, J. Bernhagen, F. Vitzthum, *Nucleic Acids Res.* **2004**, *32*, e103-e103.
[25] A. I. Dragan, R. Pavlovic, J. B. McGivney, J. R. Casas-Finet, E. S. Bishop, R. J. Strouse, M. A. Schenerman, C. D. Geddes, *J. Fluoresc.* **2012**, *22*, 1189-1199.
[26] a) M. V. Keck, S. J. Lippard, *J. Am. Chem. Soc.* **1992**, *114*, 3386-3390; b) K. J. Miller, J. F. Pycior, *Biopolymers* **1979**, *18*, 2683-2719; cK. Utsuno, M. Tsuboi, *Chem. Pharm. Bull.* **1997**, *45*, 1551-1557.
[27] a) M. Maaloum, P. Muller, S. Harlepp, *Soft Matter* **2013**, *9*, 11233-11240; b) J. D. McGhee, P. H. von Hippel, *J. Mol. Biol.* **1974**, *86*, 469-489; c) S. N. Rao, P. A. Kollman, *Proc. Natl. Acad. Sci. U.S.A.* **1987**, *84*, 5735-5739.

Table of Contents

Experimental Section

Targets and Primer Sequences

The target miRNA sequences were retrieved from miRBase Sequence Database maintained by the University of Manchester (http://www.mirbase.org).[1] A total of four synthetic miRNA sequences (Table S1) were purchased from Integrated DNA Technologies, Inc. (IDT, Coralville, IA) in both RNA and DNA forms. Synthetic Luciferase Control mRNA (only RNA form) with poly(A)-tail (30 bases) was purchased from Promega Corporation, Madison, WI. The forward and reverse primers targeting different product lengths in Luciferase Control mRNA were designed (Table S2) and purchased from IDT, Coralville, IA.
All NA samples were received in lyophilized form. Each synthetic NA samples and DNA primers were constituted to a final concentration of 100 µM in nuclease-free water (Invitrogen, Carlsbad, CA). To avoid any damage to NA by repeated freeze and thaw cycles, the small sample volumes (5 µL) were aliquot in PCR tubes. The RNA samples were stored at -80°C, whereas the DNA samples and primers were kept at -20°C. All dilutions were performed in nuclease-free water.

Reverse Transcription (RT)

Based on the qPCR detection strategy i.e. SYBR Green vs TaqMan, and microRNA vs mRNA, three different kits were purchased for cDNA synthesis. The Mir-X^{TM} miRNA first-strand synthesis kit (Takara Bio USA Inc., Mountain View, CA) converted the miRNA to cDNA for SYBR Green based miRNA qPCR detection. The reaction mix included 3.75 µL of known copies of synthetic sample, 5.0 µL of mRQ Buffer, and 1.25 µL mRQ Enzyme mix (poly(A)-polymerase and SMART MMLV Reverse Transcriptase). Each RT reaction mix was incubated in T100 Thermal Cycler (Bio-Rad Laboratories, Hercules, CA) for 1 hour at 37°C, then enzymes were inactivated at 85°C for next 5 minutes. Finally, the 10 µL RT mix was diluted to 100 µL by adding nuclease-free water. The TaqMan Advanced miRNA cDNA Synthesis Kit (Applied Biosystems, Foster City, CA) required four steps to prepare cDNA for TaqMan based microRNA detection. In step 1 polyadenylation of the sample at 3' end was obtained. In this step, 2.0 µL of known copies of sample was added in 3.0 µL of poly(A) reaction mix [0.5 µL of 10X poly(A) buffer; 0.5 µL of 10mM ATP; 0.3 µL of poly(A) enzyme (5 U/µL); 1.7 µL nuclease-free water]. The total 5.0 µL was incubated in Thermal Cycler for 45 minutes at 37°C, then reaction was stopped by denaturing enzyme at 65°C for 10 minutes. In step 2, adaptor ligation at 5' end of the sample was obtained. In this step, 5.0 µL of step 1 was mixed with 10.0 µL of ligation reaction mix [3.0 µL of 5X DNA ligase buffer; 4.5 µL of 50% PEG 8000; 0.6 µL of 25X ligation adaptor; 1.5 µL of RNA ligase; 0.4 µL of nuclease-free water]. The total 15.0 µL adapter ligation mix was incubated in Thermal Cycler at 16°C for 1 hour. Step 3 was reverse transcription (RT) reaction, where 15.0 µL of step 2 mix was added to 15 µL of RT mix [6.0 µL of 5X RT buffer; 1.2 µL of dNTPs (25 mM each); 1.5 µL of 20X universal RT primer; 3.0 µL of RT enzyme (SuperScript™ III); 3.3 µL of nuclease-free water]. The total 30.0 µL of reaction was incubated in

Thermal Cycler at 42°C for 15 minutes and then the reaction was terminated at 85°C for 5 minutes. The final step 4 was miR-amp reaction, where 5.0 µL of step 3 was mixed with 45.0 µL of miR-Amp reaction mix [25.0 µl of 2X miR-Amp master mix; 2.5 µL of 20X miR-Amp primer mix; 17.5 µL of nuclease-free water]. This 50.0 µL of reaction mix was incubated in Thermal Cycler at 95°C for 5 minutes, followed by 14 cycles of 95°C for 3 seconds and 60°C for 30 seconds. The reaction was stopped at 99°C for 10 minutes.
The High-Capacity cDNA Reverse Transcription Kit (Applied Biosystems, Foster City, CA) was utilized to synthesize cDNA from Luciferase Control mRNA. In this method, a known number of copies of mRNA were added in 10.0 µl of 2X RT master mix [2.0 µL of 10X RT buffer; 0.8 µL of 25X dNTP mix (100 mM); 2.0 µL of 10X RT random primers; 1.0 µL of MultiScribe Reverse Transcriptase; 1.0 µL of RNase inhibitor; 3.2 µL of nuclease-free water]. The 20 uL of total volume was then incubated in Thermal Cycler at 25°C for 10 minutes, 37°C for 2 hours, and 85°C for 10 minutes. Special attention was given to prepare fresh cDNA for any given qPCR experiment and avoid freeze and thaw limitations.

Quantitative PCR

All qPCR reactions, including no template control (NTC), were run in triplicates on Applied Biosystems QuantStudio 3 qPCR machine. To avoid any manual and pipetting error, a master mix without cDNA was prepared, distributed in 96-well plate, and then respective amounts of cDNA was added to the corresponding wells. Nuclease-free water was used for NTC.
Mir-X miRNA qRT-PCR SYBR kit (Takara Bio USA Inc., Mountain View, CA) was purchased for SYBR Green based qPCR detection of microRNA. The mature sequence of miRNA in the form of DNA oligo was used as 5' primer. The 3' primer (mRQ 3' Primer) was universal for all miRNA and supplied with the kit. The 0.8 uL of cDNA synthesized by Mir-X^{TM} miRNA first-strand synthesis kit (Takara Bio USA Inc., Mountain View, CA) (as discussed above) was added to aliquot master mix qPCR reaction in a 96-well plate with components: 5.0 µL of 2X SYBR Advantage Premix; 0.2 µL of 50X ROX dye; 0.2 µL of miRNA specific 5' primer; 0.2 µL of mRQ 3' primer; 0.8 uL of cDNA; and 3.6 µL of nuclease-free water. The final volume of each reaction mix was 10.0 µL. The 96-well plate was incubated in qPCR machine with following settings: 95°C for 10 seconds, 40 cycles of qPCR at 95°C for 5 seconds followed with 60°C for 20 seconds, and a final incubation for melt curve analysis at 95°C for 60 seconds, 55°C for 30 seconds, and 95°C for 30 seconds.
Because, TaqMan assays are specific to miRNA sequences due to sequence-specific TaqMan probes, unlike SYBR Green assays that can detect any microRNA, three TaqMan Advanced miRNA Assay kits (Applied Biosystems, Foster City, CA) were purchased to specifically detect miR-141, miR-155 and miR-630, respectively. A 10.0 µL of qPCR reaction was set for each miRNA in triplicate in 96 well plate. The components of reaction mix include 5.0 µL of 2X TaqMan Fast Advanced Master Mix; 0.5 uL of miRNA specific 20X TaqMan Advanced miRNA assay; 2.5 uL of 1:10 times diluted cDNA synthesized using TaqMan Advanced miRNA cDNA Synthesis Kit (Applied Biosystems, Foster City,

CA); and 2.0 uL of nuclease-free water. The loaded 96 well plate was then incubated in qPCR machine with following incubation steps: 95°C for 20 seconds, followed by 40 cycles of 95°C for 1 second and 60°C for 20 seconds. Luciferase Control mRNA standard curves were prepared by PowerUp SYBR Green Master mix (Applied Biosystems, Foster City, CA). The components of reaction mix were: 5.0 µl of 2X PowerUp SYBR Green master mix; 0.5 µL of 10.0 µM forward primer (SI Table S2); 0.5 µL of 10.0 µM of reverse primer (SI, Table S2); 1.0 µL of cDNA prepared by High-Capacity cDNA Reverse Transcription Kit (Applied Biosystems, Foster City, CA); and 3.0 µL of nuclease-free water. The qPCR mix in 96 well plate was then incubated in qPCR machine with settings: 50°C for 2 minutes, 95°C for 2 minutes, followed by 40 cycles of 95°C for 15 seconds, 55-60°C (based on Tm of primer set as in SI Table S2) for 15 seconds, and 72°C for 1 minute. A melt curve cycle was included with settings of 95°C for 15 seconds, 60°C for 1 minute, and 95°C for 15 seconds.
The qPCR data was analyzed with QuantStudio Design & Analysis Software v1.4 (Applied Biosystems, Foster City, CA). The baseline and threshold values were kept constant to avoid any batch-to-batch inconsistencies in qPCR data.

Table S1. Details of human miRNA used in the study.

miRNA	Sequence	GC %	Tm (°C)	Importance	References
miR-34a	UGGCAGUGUCUUAGCUGGUUGU	50.0	58.8	Biomarker, Cancer, Senescence	[2]
miR-141	CAUCUUCCAGUACAGUGUUGGA	45.5	54.3	Biomarker, Cancer, Melanogenesis, Chemotherapy	[3]
miR-155	UUAAUGCUAAUCGUGAUAGGGGUU	37.5	53.9	Biomarker, Immune Thrombocytopenia, Cancer, Autophagy	[4]
miR-630	AGUAUUCUGUACCAGGGAAGGU	45.5	54.9	Biomarker, Cancer, Apoptosis, Chemotherapy	[5]

Table S2. qPCR primers to target different sizes of product in luciferase control mRNA.

PCR Primer	Primer Sequence	Product length (bp)	GC %	Tm (°C)
	Primer Set 1			
P1 Luc Forward	TTTTTTATGGAAGACGCCA	40	36.8	49.7
P1 Luc Reverse	CGCCGGGCCTTTCTTTATG		57.9	56.7
	Primer Set 2			
P2 Luc Forward	TGAACATCACGTACGCGG	44	55.6	55.3
P2 Luc Reverse	CCGAACCAAGGACATTTCGAAG		50	56.2
	Primer Set 3			
P3 Luc Forward	AGATCGTGGATTACGTCGCC	57	55	57
P3 Luc Reverse	CTCCTCCGCGCAACTTTTTC		55	57
	Primer Set 4			
P4 Luc Forward	TACAACACCCCAACATCTTCGA	67	45.5	56.2
P4 Luc Reverse	GGAAGTTCACCGGCGTCAT		57.9	57.9
	Primer Set 5			
P5 Luc Forward	CCGAGGGGGATGATAAACCG	109	60	57.5
P5 Luc Reverse	TCGCCTCTCTGATTAACGCC		55	57
	Primer Set 6			
P6 Luc Forward	TTACACCCGAGGGGGATGAT	242	55	57.8
P6 Luc Reverse	GTGTTCGTCTTCGTCCCAGT		55	57.1

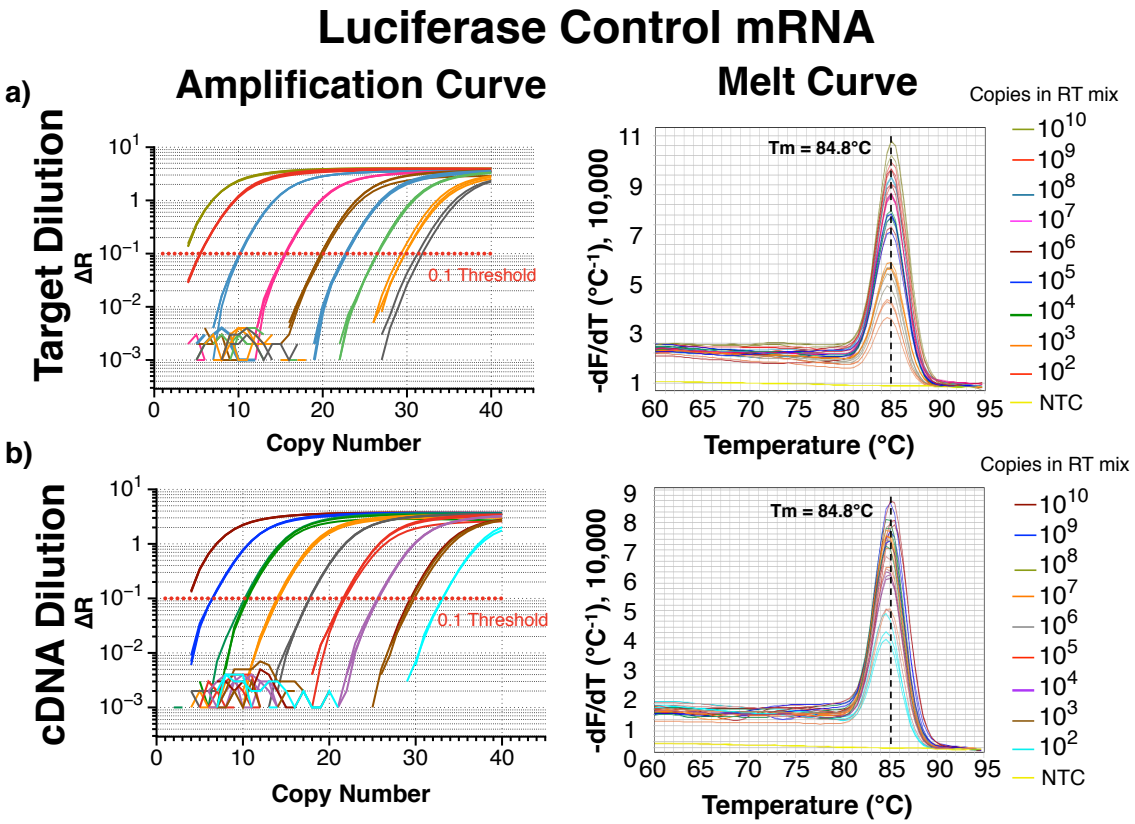

Figure S1. The SYBR Green qPCR amplification and melt curves for Luciferase Control mRNA for a) target dilution, and b) cDNA dilution. The statistical analysis of amplification plots and one peak in the melt curve reflect the reliability of the qPCR data.

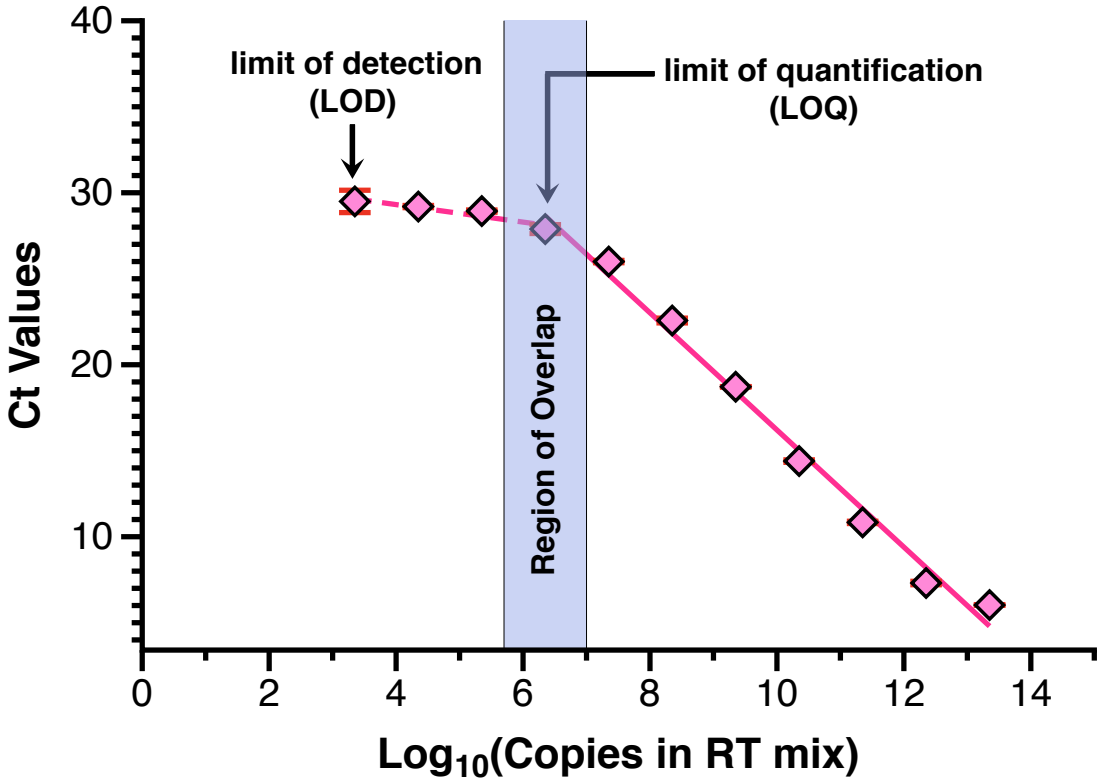

Figure S2. A typical SYBR Green qPCR based miRNA standard curve with limit of detection (LoD) and limit of quantification (LoQ). This standard curve is generated by target dilution of miR-155 RNA synthetic sequence. In this case, miR-155 has a quantification limit of ~10^6 copies in RT mix (equivalent to 1 pM in a sample) and a detection limit for miR-155 is ~10^3 copies in RT mix (equivalent to [c] ~ 1 fM in a sample). The "Region of Overlap" represents the area where quantification curve switch to a plateau.

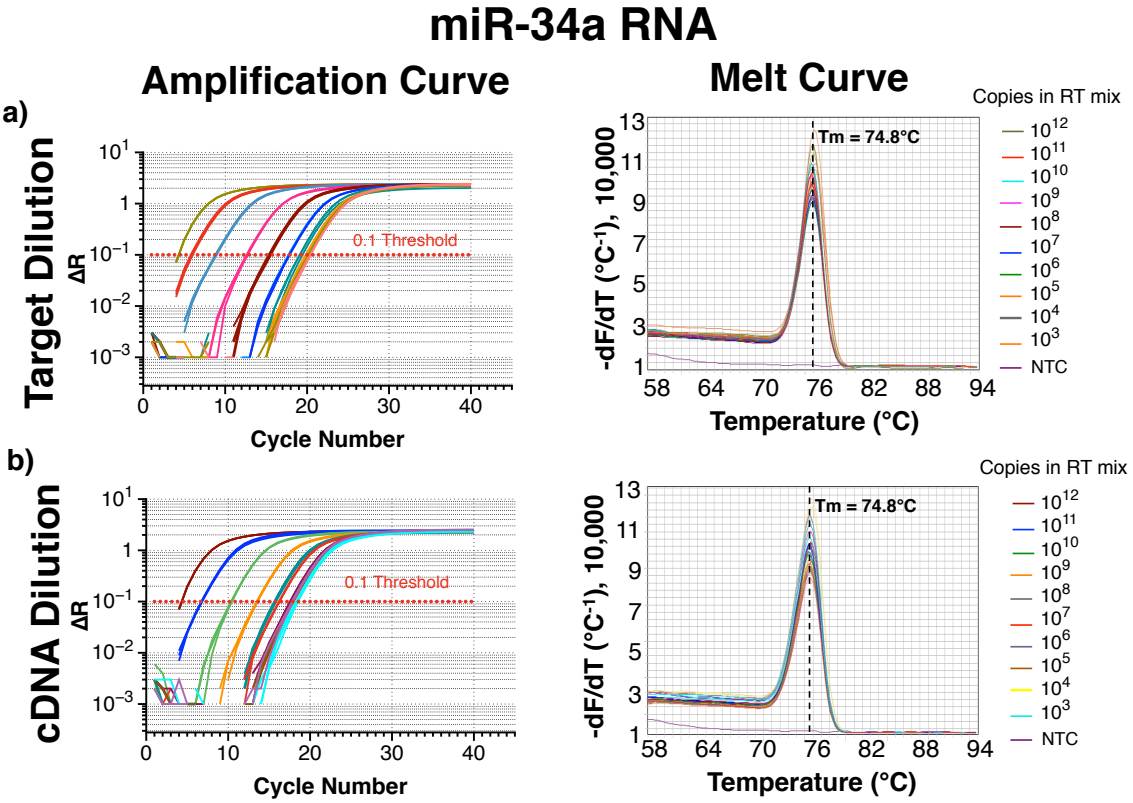

Figure S3. The SYBR Green qPCR amplification and melt curves for miR-34a RNA for a) target dilution, and b) cDNA dilution. The statistical analysis of amplification plots and one peak in the melt curve reflect the reliability of the qPCR data.

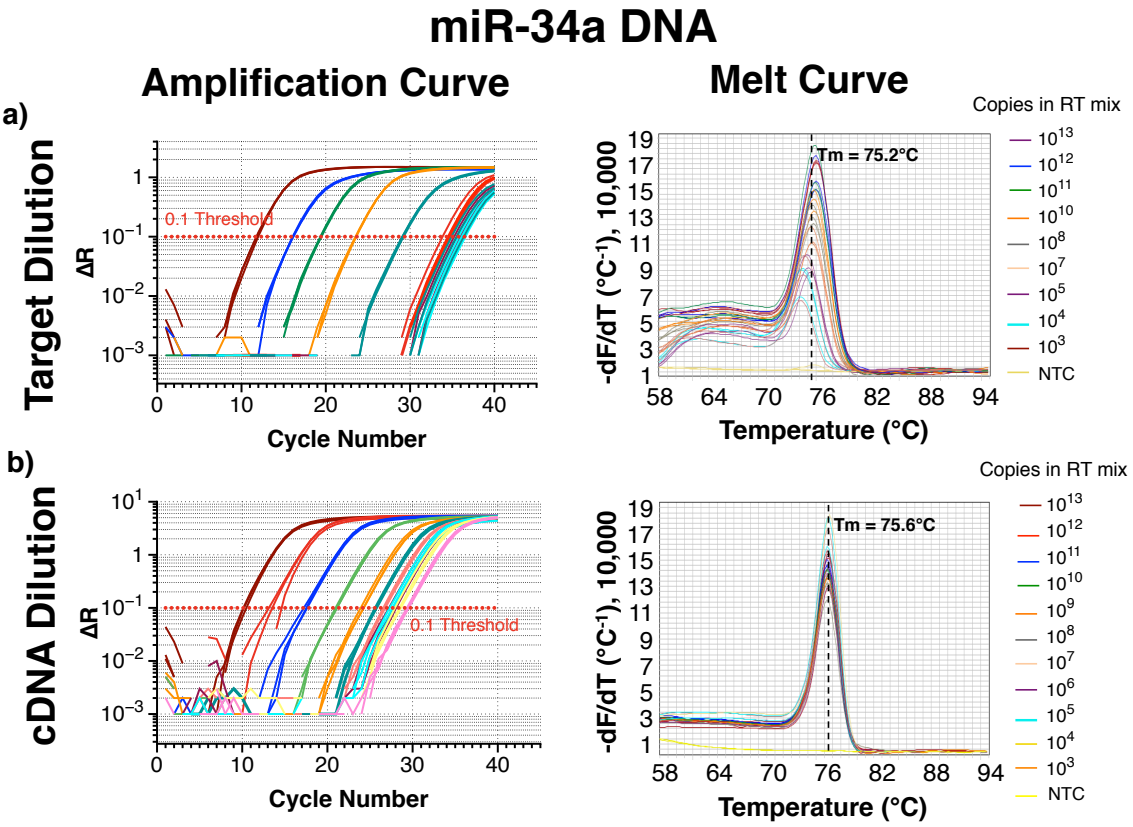

Figure S4. The SYBR Green qPCR amplification and melt curves for miR-34a DNA for a) target dilution, and b) cDNA dilution. The statistical analysis of amplification plots and one peak in the melt curve reflect the reliability of the qPCR data.

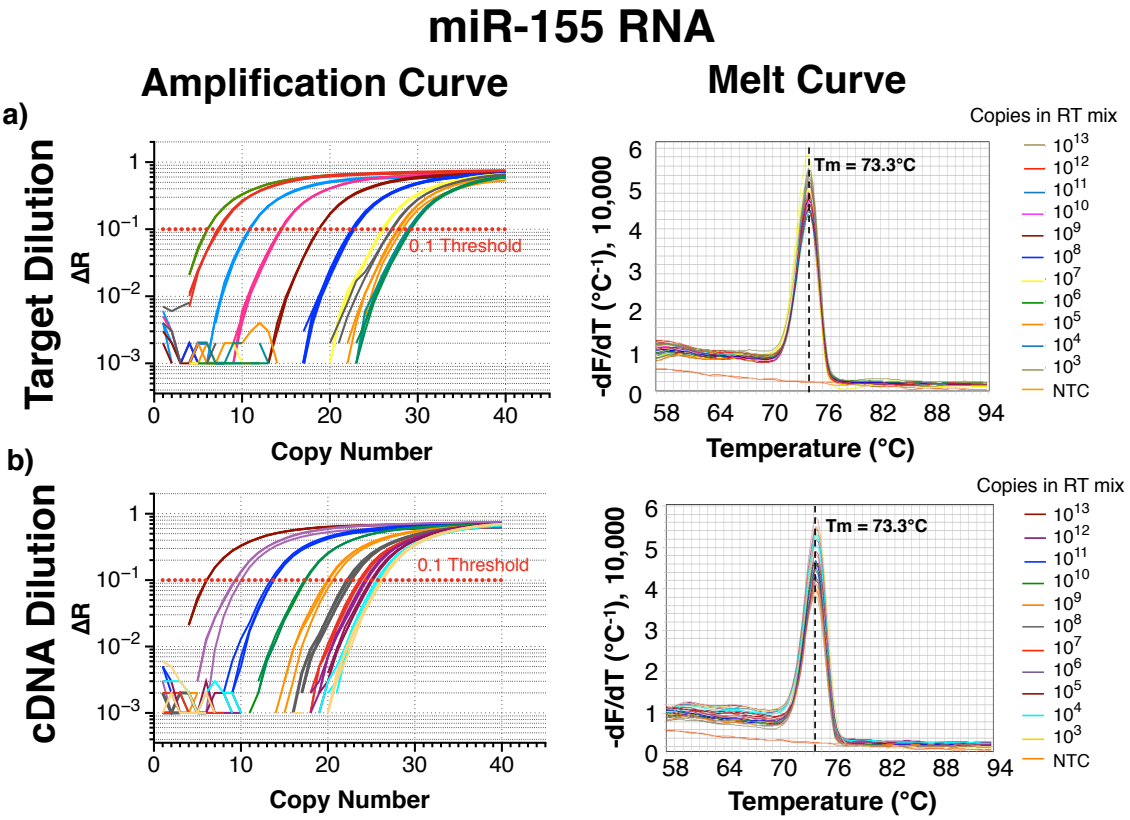

Figure S5. The SYBR Green qPCR amplification and melt curves for miR-155 RNA for a) target dilution, and b) cDNA dilution. The statistical analysis of amplification plots and one peak in the melt curve reflect the reliability of the qPCR data.

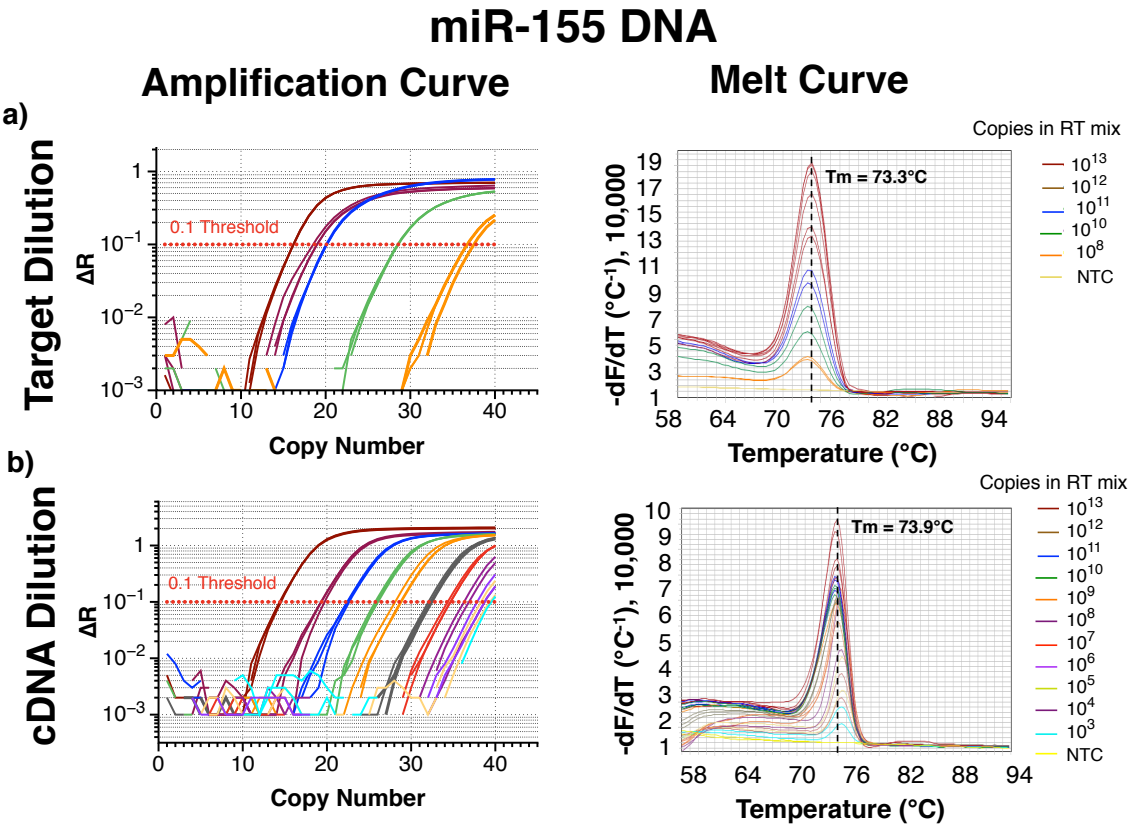

Figure S6. The SYBR Green qPCR amplification and melt curves for miR-155 DNA for a) target dilution, and b) cDNA dilution. The statistical analysis of amplification plots and one peak in the melt curve reflect the reliability of the qPCR data.

References

[1] S. Griffiths-Jones, R. J. Grocock, S. van Dongen, A. Bateman, A. J. Enright, *Nucleic Acids Res.* **2006**, *34*, D140-D144.

[2] a) L. Baronti, I. Guzzetti, P. Ebrahimi, S. Friebe Sandoz, E. Steiner, J. Schlagnitweit, B. Fromm, L. Silva, C. Fontana, A. A. Chen, K. Petzold, *Nature* **2020**, *583*, 139-144; b) T. Chen, J. Yan, Z. Li, *Mutat*. *Res*. **2020**, *856-857*, 503232; c) H. Hermeking, *Cell Death Differ.* **2010**, *17*, 193-199; d) N. Mokhberian, Z. Bolandi, M. Eftekhary, S. M. Hashemi, V. Jajarmi, K. Sharifi, H. Ghanbarian, *Life Sci*. **2020**, *257*, 118055; e) C. Welch, Y. Chen, R. L. Stallings, *Oncogene* **2007**, *26*, 5017-5022.

[3] a) T. Itoh, K. Fukatani, A. Nakashima, K. Suzuki, *Sci. Rep.* **2020**, *10*, 2149; b) G. Lu, Y. Zhang, *PLoS One* **2020**, *15*, e0229118; c) F. Meng, R. Henson, M. Lang, H. Wehbe, S. Maheshwari, J. T. Mendell, J. Jiang, T. D. Schmittgen, T. Patel, *Gastroenterology* **2006**, *130*, 2113-2129; d) F. Wang, J. X. Yang, Z. N. Chen, *Zhonghua Zhong Liu Za Zhi* **2020**, *42*, 556-559; e) Y. Ye, X. H. Yuan, J. J. Wang, Y. C. Wang, S. L. Li, *Medicine* **2020**, *99*.

[4] a) Y. Chang, X. Chen, Y. Tian, X. Gao, Z. Liu, X. Dong, L. Wang, F. He, J. Zhou, *Life Sci.* **2020**, *257*, 118057; b) X. Chen, X. B. Zhang, D. J. Li, G. N. Qi, Y. Q. Dai, J. Gu, M. Q. Chen, S. Hu, Z. Y. Liu, Z. M. Yang, *Exp. Mol. Pathol.* **2020**, *115*, 104450; c) W. Tam, J. E. Dahlberg, *Genes Chromosomes Cancer* **2006**, *45*, 211-212.

[5] a) D. Chu, Z. Zhao, Y. Li, J. Li, J. Zheng, W. Wang, Q. Zhao, G. Ji, *PLoS One* **2014**, *9*, e90526; b) K. J. Eoh, S. H. Lee, H. J. Kim, J.-Y. Lee, S. Kim, S. W. Kim, Y. T. Kim, E. J. Nam, *Biochem. Biophys. Res. Commun.* **2018**, *497*, 513-520; c) L. Farhana, M. I. Dawson, F. Murshed, J. K. Das, A. K. Rishi, J. A. Fontana, *PloS one* **2013**, *8*, e61015-e61015; d) Y. H. Li, C.L. Xu, C. J. He, H. H. Pu, J.L. Liu, Y. Wang, *Mol. Carcinog.* **2020**, *59*, 141-153; e) X. M. Pan, X. Y. He, Y. L. Yang, W. J. Jia, Z. Q. Yang, D. Yan, J. X. Ma, *Eur. Rev. Med. Pharmacol. Sci.* **2019**, *23*, 2453-2460.